Appl. Phys. A 89, 293–297 (2007)
DOI: 10.1007/s00339-007-4125-3

Applied Physics A
Materials Science & Processing

L. WANG
X. XU✉

Spectral resonance of nanoscale bowtie apertures in visible wavelength

School of Mechanical Engineering, Purdue University, West Lafayette, IN 47907, USA

Received: 29 March 2007 / Accepted: 2 May 2007
Published online: 21 June 2007 • © Springer-Verlag 2007

ABSTRACT We report spectroscopic measurements of transmitted field through bowtie-shaped nanoscale apertures in visible wavelength region. Resonance in these apertures and its relation with the aperture geometry are investigated. The near-field spectral response is also investigated using finite difference time domain (FDTD) computation and compared with the spectroscopic measurements. The dependences of the peak wavelength and peak amplitude on the geometry of the bowtie aperture are illustrated. Design rules are proposed to optimize the bowtie aperture for producing a sub-wavelength, high transmission field.

PACS 81.07.-b; 07.79.Fc; 71.36.+c; 78.66Bz; 42.79.Gn; 42.79.Vb

1 Introduction

Light transmission through a nanoscale aperture in a metallic film allows a confined spot to be produced in the near field. Producing a nanoscale light spot has drawn much attention in recent years as a nanoscale light spot can be used in many applications requiring high spatial resolution such as single molecule detection [1], nanofabrication [2] and high density data storage [3]. However, using a simple nanometer-sized hole in circular or square shapes is plagued by its low transmission and poor contrast [4]. The low transmission through regular nanoapertures can be ascribed to the waveguide cutoff effect. It is known that the fundamental cutoff wavelengths for the waveguides with circular and square cross sections are $1.7d$ and $2d$, where d is the diameter of the circular waveguide or the side length of the square waveguide, respectively. A sub-100 nm circular hole will be subjected to the cutoff conditions under UV or visible light illumination; therefore, light cannot be efficiently coupled through. This drawback limits regular nanoapertures from being employed in many applications.

Many efforts have been made to improve the transmission efficiency through sub-wavelength apertures while maintaining their near-field confinement function. One approach is to take advantage of the enhancement of localized surface plasmon by introducing a minute scatter in the center of a regular aperture [5]. Although this approach promises sub-diffraction-limited resolution, sub-100 nm near-field radiation is yet to be demonstrated [6]. Another approach follows the similar mechanism of transmission enhancement through a hole array in noble metal films [7] or using a circular aperture surrounded by a periodic ring corrugations (bull's eye pattern) [8] so that the transmission can be enhanced at selected resonant wavelengths.

Recently, it is demonstrated that high transmission efficiency and confined nanoscale radiation can be obtained simultaneously by using nanoscale bowtie aperture [9–11]. Compared to regularly shaped nanoapertures, it has been numerically and experimentally demonstrated that bowtie apertures are capable of providing a nanometer-size near-field spot as well as enhanced transmission orders of magnitude higher than regularly shaped apertures [9–11]. The unique properties of bowtie nanoapertures as shown in Fig. 1 are endowed by their specially designed geometries: two open arms and a nanometer-size gap. When illuminated by an excitation source with proper polarization – in the direction across the gap, the open arms allow longer cutoff wavelengths while the gap size determines the size of the transmitted light spot. The transmitted field through the bowtie apertures is not only confined, but also greatly enhanced compared to regular nanoapertures operated under the cutoff conditions. Utilizing these apertures in the visible regime, however, presents several design, fabrication, and experimental challenges. In this report we study the resonance of bowtie apertures in the visible region. Bowtie apertures with various shapes are investigated using both spectral measurements and numerical methods, and the results of spectral measurements and calculations are compared.

2 Experimental approach

Bowtie apertures were fabricated using an FEI Strata DB 235 FIB (focused ion beam) tool. A cleaned 150-mm-thick aluminum film was deposited on quartz wafer by e-beam deposition. The apertures were then formed in the aluminum film by ion milling with 30 keV focused Ga^+ ions at 1 pA beam current. The gap size should be as small as possible because the light spot produced by the bowtie aperture is determined by its gap size [9]. However, the smallest gap size

✉ Fax: 1-765-494-0539, E-mail: xxu@ecn.purdue.cn

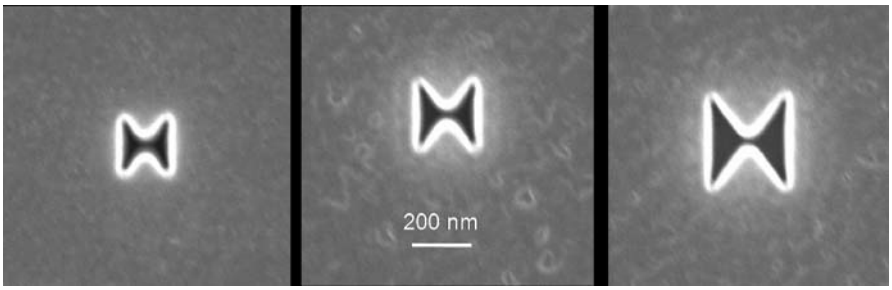

FIGURE 1 SEM pictures of fabricated bowtie apertures

that can be practically fabricated using our FIB tool is about 30 nm due to the limitations of finite ion beam size. Thin aluminum film of 150 nm thick is selected because of its small skin depth and high reflectivity. SEM pictures of three bowtie apertures of 180 nm, 200 nm, and 280 nm outline dimension and a same gap size of 33 nm are shown in Fig. 1.

Investigation of the spectral responses of nanoapertures is important for understanding their behavior [7, 8, 12], and would allow determination of the resonance wavelength and optimization of their performance for a tailored application. Figure 2 shows a simplified schematic of the experimental setup used in this work for the far-field spectral transmission measurement. A tunable laser output from an optical parametric amplifier (OPA) pumped by an amplified ultrafast laser system is used as the light source. The laser beam is focused onto the sample using a condenser lens with numerical aperture NA = 0.15. The transmitted laser light through nanoapertures in the sample is collected by a 50× objective and directed onto a photomultiplier tube. To collect single-aperture transmission, a 50 μm pinhole was placed in the image plane of the objective, defining the spatial resolution of about 1 μm. The individual apertures were spaced 15 μm apart to limit coupling among apertures, and to ensure that transmitted light was collected solely from one aperture. The sample was raster scanned, and recorded by the PMT signal readout. The power throughput of each nanoaperture in different wavelengths can therefore be compared by the photon counts after spectral calibration.

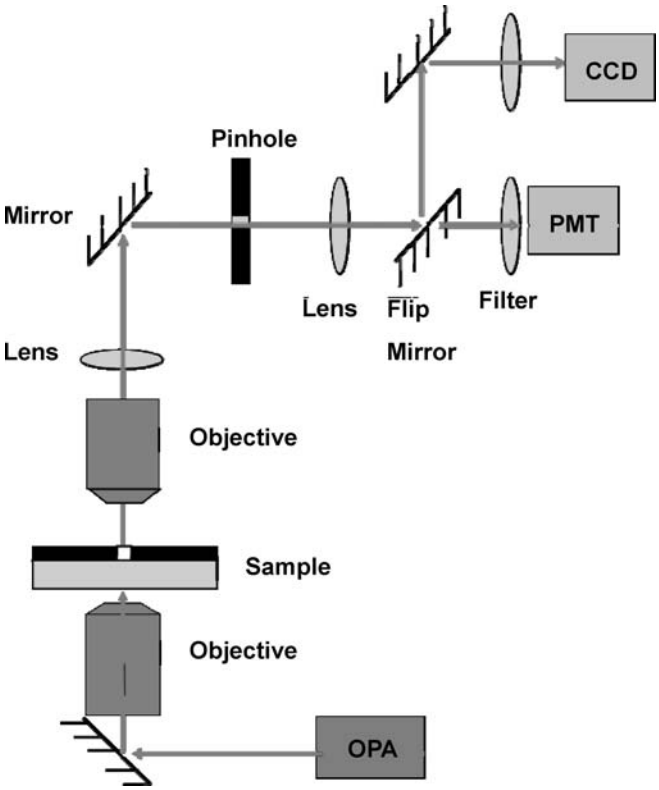

FIGURE 2 Schematic diagram of far field measurement setup

3 Simulation

It is well known that Fourier optics is no longer adequate for analyzing optical properties and responses in real metals due to the finite skin depth, film thickness, and possible surface plasmon effect [13]. Instead, vigorous vectorial analysis must be applied. The finite difference time domain – FDTD numerical method first introduced by Yee in 1966 [14] can be used to simulate the optical near filed of light transmission through subwavelength apertures by numerically solving the Maxwell's equations. In the FDTD algorithm, the computational region is discretized into small cubes, called Yee cells. Each cell has a dimension of Δx, Δy, and Δz in Cartesian coordinates with size less than tenth of wavelength to ensure accurate numerical results. However, in the study of the near field of nanostructures, the cell size should be much smaller than the smallest dimensions of nanostructures to ensure the physical convergence, especially when the field quantities in the vicinity of the nanostructure is of interest. In this work $4 \times 4 \times 4\,\mathrm{nm}^3$ cells are used to model bowtie nano-apertures. The stability condition relating the spatial and temporal step size is used, which is expressed as

$$v_{\max}\Delta t = \left[\frac{1}{\Delta x^2} + \frac{1}{\Delta y^2} + \frac{1}{\Delta z^2}\right]^{-1/2}, \tag{1}$$

where $v_{\max}$ is the maximum velocity of the wave in the material. In addition, absorbing or perfectly matched boundary conditions [15, 16] are employed to eliminate the reflected waves on the boundaries of the finite computational domain. The second-order absorbing boundary condition [16] is used in this work. The commercial software package XFDTD 5.3 from Remcom is used, which has been used in many near field calculations [9, 10].

The modified Debye model is used to compute the complex permittivity for aluminum, which is expressed as

$$\varepsilon(\omega) = \varepsilon_\infty + \frac{\varepsilon_\mathrm{s} - \varepsilon_\infty}{1 + j\omega\tau} + \frac{\sigma}{j\omega\varepsilon_0}, \tag{2}$$

where ε_s represents the static permittivity, ε_∞ is the permittivity at infinite frequency which should be no less than 1, σ

is conductivity, and τ is the relaxation time. Given the experimental refractive index data of aluminum in the wavelength range of interest [17], the parameters in the Debye model are found as $\varepsilon_\infty = 1$, $\varepsilon_s = -507.825$, $\tau = 9.398 \times 10^{-16}$ s, and $\sigma = 4.8 \times 10^6$ s/m. The simulated geometry consists of a 150 nm thick aluminum film and a semi-infinite quarts layer. The wavelength of incident light varies from 400 nm to 800 nm and the polarization of the light is in the direction across the gap of bowtie apertures. The index of refractive used for the quartz is 1.5.

4 Results and discussion

It is well known that light scattering of metallic nanoparticles and apertures have strong geometry dependence [5–7]. In this report we focus our study on the resonance in the visible wavelength range. Figure 3 shows the measured transmission through three bowtie apertures of different outline sizes: 180 nm, 200 nm and 280 nm as a function of the illumination wavelength. A resonant peak is found in the visible wavelength range for all three apertures. The trend of the spectrum response also indicates that there is another resonant peak in the near infrared region. However, this second resonant peak is not be measured since our experimental system only provides the wavelength range as indicated in Fig. 3, which is limited by the response of the photomultiplier tube. From the figure it can be seen that the larger bowtie aperture has a resonant peak at longer wavelength, indicating the red shift of the resonant wavelength with respect to the bowtie aperture outline dimension. In addition, the amplitude of the peak response also increases as the aperture outline dimension increases. This is simply because more light is able to be coupled through for a larger aperture.

Far-field and near-field spectra of a 180 nm bowtie aperture with a 32 nm gap are simulated and normalized to its peak value as shown in Fig. 4. The far field is calculated as the integral of the transmitted power at a distance 300 nm from the aperture exit; whereas the near field is the intensity at at the center of the aperture on the exit plane. From the figure it is found that the far-field and near-field spectra have the same resonant wavelength and follow the same trend, but the far field transmission is slightly lower than the near field transmission at longer wavelengths. Figure 5 compares the calculated near-field spectra of three bowtie apertures of the same dimensions as experimentally measured apertures. Comparing the calculated results with the measurement data, it can be seen that the simulated spectral curves follow the same trend as the experimental results: there is a resonant peak in the visible wavelength range for each aperture, and there is also a resonance peak in the infrared range as seen from the trend of the calculated curve. The numerical calculation also predicts a red shift when the bowtie aperture size increases. On the other hand, the resonant positions of the calculated and measured resonance peaks do not exactly coincide with each other, which can be due to the difficulties in precisely measuring and modeling the actual aperture dimensions and the inaccuracy in the optical properties of the material.

The calculated amplitude of the peak response increases as the aperture outline size increase, which is also predicted by the experimental results. FDTD simulated field intensity distribution of 180 nm outline dimension bowtie aperture with 32 nm gap size at the resonant wavelength of 525 nm is shown in Fig. 6a, showing a strong field at the exit of the aperture. On the other hand, as shown in Fig. 6b at the non-resonant wavelength of 400 nm, the light intensity is much smaller. At the resonance, the aperture acts as a resonant cavity and provides the most efficient transmission from the entrance to the exit.

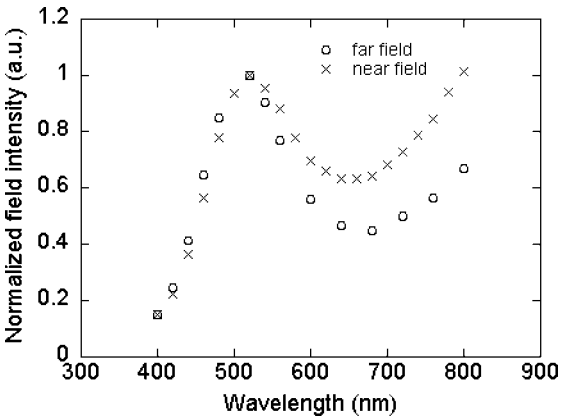

FIGURE 4 The far-field and near-field transmission spectra of bowtie apertures with outline of 180 nm

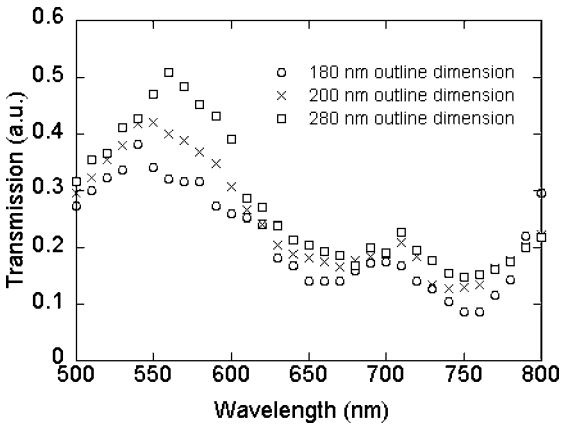

FIGURE 3 Power throughput of bowtie apertures of three different sizes in 150 nm aluminum film as a function of illumination wavelength

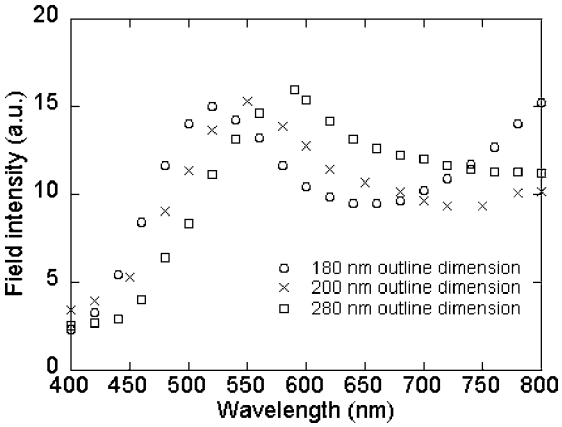

FIGURE 5 The near-field spectra of bowtie apertures in various outline sizes: 180 nm, 200 nm and 280 nm

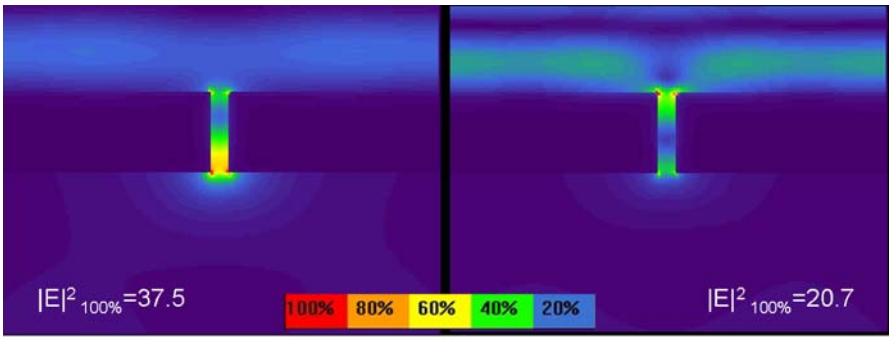

FIGURE 6 FDTD simulated field intensity distribution of the 180 nm outline dimension bowtie aperture with 32 nm gap size at the excitation wavelengths of (**a**) 525 nm (resonance) and (**b**) 400 nm (non-resonance)

The calculated shortest resonant wavelength as a function of the outline dimension is further illustrated in Fig. 7. A 120 nm outline size bowtie aperture with a 32 nm gap was also simulated. A linear relation can be seen in the figure, with a 0.75 nm red-shift of the resonant wavelength per 1 nm increase in the aperture size. Practically, due to the fabrication limitations the smallest outline size of bowtie aperture that can be fabricated is about 150 nm. Therefore the shortest wavelength that the resonant peak can occur is about 503 nm. On the other hand, in order to obtain the confined light, the outline size of the bowtie aperture has to be less than about half of the wavelength so that transmission is confined within the gap. Calculations show that when the wavelength is larger than 608 nm, the outline dimension becomes larger than the half wavelength. This leads to a maximum resonant wavelength of about 608 nm.

To illustrate the effect of the gap size of the bowtie aperture, the near-field spectra of bowtie apertures with various gap sizes are also calculated and shown in Fig. 8. Three gap sizes of 24 nm, 32 nm and 48 nm are compared. The other dimensions for the three bowtie apertures are kept the same: 200 nm outline dimension, and 152 nm film thickness. It can be seen that resonant wavelength does not change with the gap size. This indicates that the resonant cavity which provides the most efficient transmission is decided by the outline dimension of the bowtie aperture. However, it is found that the field intensity becomes stronger at the smaller gap size. The transmitted field can be considered as induced by the dipole radiation at the two bowtie tips. As the gap size reduces, the charge density increases due to the stronger coupling between the two tips and the near-field strength therefore increases.

Based on the above results, we can obtain the design rules for achieving both high transmission and high resolution in the visible wavelength range. First, the gap size needs to be fabricated as small as possible to achieve the best resolution which also helps to increase the near field transmission. The smallest gap size can be fabricated by FIB tool is about 30 nm. Then for wavelength range between 503 and 608 nm, the outline dimension can be fabricated to achieve resonant transmission. However, for other wavelengths since resonant condition cannot be met, its outline dimension needs to be tuned to find the maximum transmitted field. As an example, Fig. 9 shows

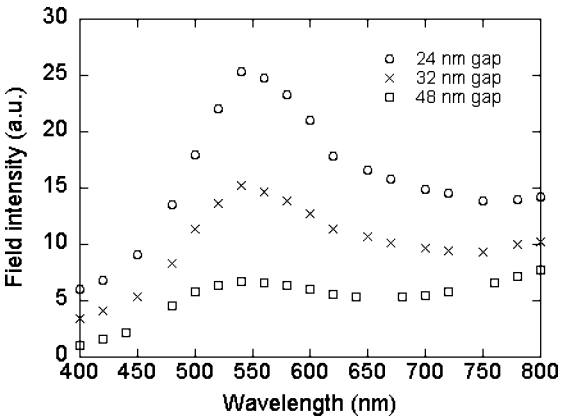

FIGURE 8 The near-field spectra of bowtie apertures in various gap width: 24 nm, 32 nm and 48 nm gap

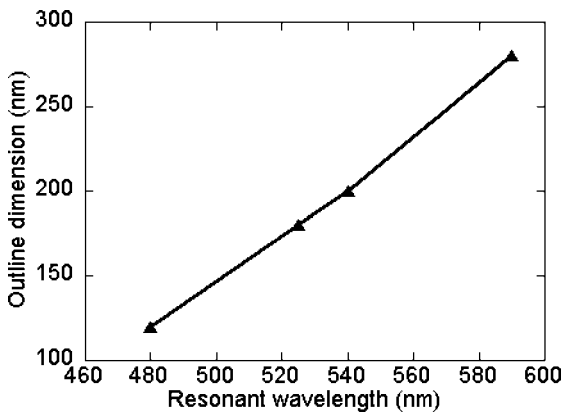

FIGURE 7 The change of resonant wavelength as a function of the outline size of bowtie aperture

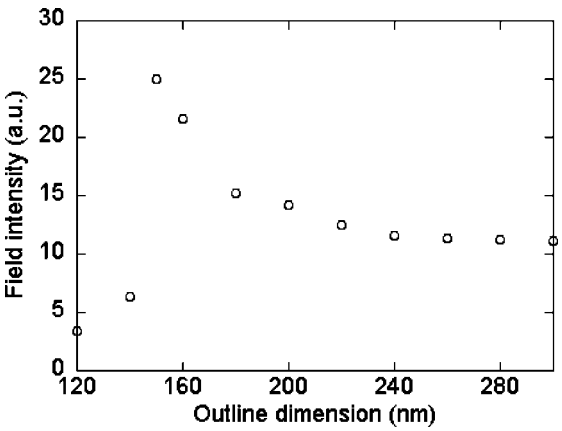

FIGURE 9 The near-field intensity of bowtie apertures in various outline dimensions at 800 nm incident wavelength

the transmission intensity as a function of outline size when the gas size fixed at 32 nm and the wavelength is at 800 nm. It is found that the maximum transmitted field occurred at a 150 nm outline dimension.

5 Conclusion

In summary, spectroscopic measurements of light transmission through bowtie-shaped apertures fabricated in aluminum film are performed. The spectral responses of three bowtie apertures of different outline dimensions and same gap size are experimentally obtained using a polarized tunable laser as the excitation source. Resonant far-field transmission is observed and the resonance is red-shifted when the overall size of the bowtie aperture increases. FDTD numerical computations are conducted and the near-field radiation spectra show similar trend as the far-field radiation measurement. We also found that the resonance does not change as the gap size between two bowtie tips decreases, but the amplitude of the near-field resonant response increases when the gap size decreases. For wavelength between about 500 and 600 nm, the bowtie aperture can be fabricated to match a desired resonance wavelength. For other wavelengths, the size of bowtie apertures can be tuned to find the highest transmission.

ACKNOWLEDGEMENTS The financial support to this work by the Nation Science Foundation is acknowledged. Fabrications of aperture samples and NSOM probes by FIB were carried out at the Birck Nanotechnology Center, Purdue University.

REFERENCES

1 E. Betzig, R.J. Chichester, Science **262**, 1422 (1993)
2 I.I. Smolyaninov, D.L. Mazzoni, C.C. Davis, Appl. Phys. Lett. **67**, 3859 (1995)
3 E. Betzig, J.K. Trautman, R. Wolfe, E.M. Gyorgy, P.L. Finn, M.H. Kryder, C.H. Chang, Appl. Phys. Lett. **61**, 142 (1992)
4 H. Bethe, Phys. Rev. **66**, 163 (1944)
5 K. Tanaka, T. Ohkubo, M. Oumi, Y. Mitsuoka, K. Nakajima, H. Hosaka, K. Itao, Japan. J. Appl. Phys. **40**, 1542 (2001)
6 K. Tanaka, H. Hosaka, K. Itao, M. Oumi, T. Niwa, T. Miyatani, Y. Mitsuoka, K. Nakajima, T. Ohkubo, Appl. Phys. Lett. **86**, 83 (2003)
7 T. Ebbesen, H. Lezec, H. Ghaemi, T. Thio, P. Wolff, Nature **391**, 667 (1998)
8 H. Lezec, A. Degiron, E. Devaux, R. Linke, L. Martín-Moreno, F. García-Vidal, T. Ebbesen, Science **297**, 820 (2002)
9 E.X. Jin, X. Xu, Japan. J. Appl. Phys. **43**, 407 (2004)
10 E.X. Jin, X. Xu, Appl. Phys. Lett. **86**, 111 106 (2005)
11 L. Wang, S.M. Uppuluri, E.X. Jin, X. Xu, Nano Lett. **6**, 361 (2006)
12 J.A. Matteo, D.P. Fromm, Y. Yuen, P.J. Schuck, W.E. Moerner, L. Hesselink, Appl. Phys. Lett. **85**, 648 (2004)
13 J.W. Goodman, *Introduction to Fourier Optics* (McGraw-Hill, New York, 1996)
14 K. Yee, IEEE Trans. Antennas Propag. **14**, 302 (1966)
15 G. Mur, IEEE Trans. Electromagn. Compatibility **23**, 377 (1981)
16 Z.P. Liao, H.L. Wong, B. Yang, Y. Yuan, Sci. Sin. **28**, 1063 (1984)
17 D.R. Lide, *CRC Handbook of Chemistry and Physics*, 77th edn. (CRC Press, Roca Raton, 1996), p. 12